ISSN 0023-1584, Kinetics and Catalysis, 2009, Vol. 50, No. 5, pp. 741–747. © Pleiades Publishing, Ltd., 2009.

High-Power Ultrasonic-Assisted Phenol and Dye Degradation on Porous Manganese Oxide Doped Titanium Dioxide Catalysts[1]

R. Jothiramalingam, T. M. Tsao, and M. K. Wang

Department of Agricultural Chemistry, National Taiwan University, Taipei, Taiwan, 106

e-mail: drjothiramalingam@yahoo.co.in, mkwang@ntu.edu.tw

Received August 6, 2008

Abstract—In this study, a high-power ultrasonicator (600 W) is employed to examine dye degradation and phenol decomposition efficiencies in the presence of catalysts such as K-OMS-2, TiO_2, K-OL-1 doped TiO_2 and K-OMS-2 doped TiO_2. Methylene blue and phenol are chosen as the model pollutants to test the catalytic activity. Effects of ultrasonic power level or ultrasonic intensity, amount of catalysts used and ultrasonic irradiation time for catalytic degradation and removal of phenol were studied. No *d*-spacing peak shift was observed in intense XRD peaks of K-OMS-2- and K-OL-1-doped TiO_2 materials when compared with commercial TiO_2. Scanning and transmission electron micrographs (SEM and TEM) show aggregated particle morphology with spherical and rectangular particles for 5 wt % K-OMS-2/TiO_2. Methylene blue dye degradation efficiency in the presence of catalytic ultrasonication follows the order like TiO_2 > 5 wt % K-OMS-2/TiO_2 > 5 wt % K-OL-1/TiO_2. The K-OMS-2- and 5 wt % K-OMS-2-doped TiO_2 catalyst showed the best and most promising efficiency for phenol removal in ultrasonication process. K-OMS-2 shows the best phenol removal efficiency of 58% within a short duration (30 min) of catalytic ultrasonic-assisted reaction.

DOI: 10.1134/S0023158409050164

INTRODUCTION

Ultrasound and sonochemical methods have been attracting attention as an advanced degradation process for eliminating hazardous chemical substances in water and waste water [1–3]. The phenomenon of cavitation (i.e., the nucleation, growth, and collapse of small gas bubbles in liquids) is the basis of a variety of mechanical and chemical processes induced in liquids by ultrasounds [4, 5]. Very high temperatures (5000 K) and pressures (several hundred atmospheres) induced by cavitation in collapsing gas bubbles in aqueous solution lead to thermal dissociation of water molecules into H atoms and hydroxyl radicals ($^{\bullet}OH$) [6, 7]. Chemical reactions with $^{\bullet}OH$ radicals from cavitation bubbles are referred to as sonochemical reactions, which are promising for green environmental processing, such as dye degradation and toxic industrial waste water treatment. The presence of chemical oxidants like hydrogen peroxide and multivalent metal oxide catalysts further facilitates the degradation process of a shorter duration with greater efficiency [8]. Suslick and Price [9] reported the detailed application of ultrasound to nanostructure material synthesis and heterogeneous catalysis.

Metal ion doping on titanium dioxide (TiO_2) provides versatile applications for organic pollutant decomposition in sono and photo catalytic processes due to perturbation in energy level of semiconducting TiO_2 [10]. The sol-gel method that synthesizes anatase–rutile phase transformation of various amounts of Mn(II) doped TiO_2 has been reported and the effects of manganese(II) dopants on acceleration of rutile phase formation were studied [11]. Manganese oxides have been reported to be among the most efficient transition-metal oxide catalyst for catalytic disposal of various pollutants like phenol and VOCs [12, 13]; and porous manganese oxide (K-OMS-2) has also been used in selective catalytic reduction of NO*x* with NH_3 [12], CO and NH_3 adsorption [14, 15]. Porous manganese oxide such as K-OMS-2 (octahedral molecular sieve) and K-OL-1 (octahedral layer) was synthesized by the reported procedure [16, 17] and the same is doped with commercial TiO_2. Synthetic K-OMS-2 has a tunnel for structuring porous manganese oxide and its crystalline structure is the same as that for mineral cryptomelane with pore size of 4.6 Å [18], while K-OL-1 is a layered structured. Porous manganese oxide (K-OL-1 and K-OMS-2)-doped TiO_2 catalysts for photo catalytic decomposition of toluene has already been reported by our group; and reaction conditions and catalyst preparation method were found to play the important roles in photocatalytic toluene decomposition [19].

Textile dyes and other dye industries produce enormous amount of toxic waste water; and hence, it is necessary to develop advanced oxidation processes with modern technology like sono-photocatalytic methods [20, 21]. Sono-sorption removal of methylene blue from aqueous solution with and without

[1] The article is published in the original.

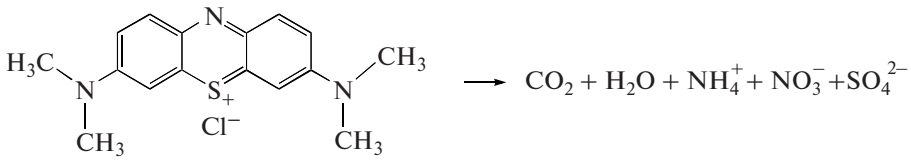

Scheme.

ultrasound using cellulosic material such as waste newspaper was examined. Degradation of methylene blue dye in the presence of ultrasound was observed within a short time due to the cavitation process, which facilitates the mass transfer and increases surface area of the sorbent [21].

Methylene blue is considered the best model pollutant for photocatalytic and sonocatalytic degradation tests in the presence of TiO_2 catalyst. In the present study, methylene blue dye degradation and phenol removal efficiency by synthesized catalysts were tested using a high-power ultrasound (600 W)-assisted ultrasonic liquid processor. The main focus of this study is to exploit the efficiency of high-power direct ultrasonic liquid process, role of catalyst and effect of reaction time in the presence of catalysts like TiO_2, K-OMS-2, K-OL-1/TiO_2 and K-OMS-2/TiO_2.

EXPERIMENTAL

Materials

Methylene blue dye was purchased from Sigma Chemical Co., Germany. Phenol from Sigma Aldrich was used without further purification. A stock solution of dye was prepared by dissolving dye in double distilled water (DDW). Manganese acetate, manganese sulphate (Acros Organics, NJ) and TiO_2 were obtained from Nacalai Tesque, Japan.

Apparatus

This study uses an ultrasonic liquid processor (Sonicator 3000) from Misonix (USA) with total output power of 600 W and frequency of 20 kHz. A standard thick titanium horn is immersed into the reactant solution for irradiation at different pulse-on and pulse-off rates. The output power levels (1–10) were specified in the sonicator. The power level should be set according to volume of the solution. In the present experiment, power levels of 4 and 8 are used for 50 ml of reactant solution (50 mg/l concentration for all experiment) in the presence of as synthesized catalyst. Power level 4 would produce intense power of 36 W (displayed on the sonicator digital screen) and power level 8 produces intense power of 66 W at the programmed pulse rate. In this study, reaction time is set to be 30 min, pulse-on time is 15 s, and pulse-off time is 10 s for all experiments.

In order to identify the crystalline phases of the as synthesized samples, Rigaku Geigerflex X-ray diffractometer was used. The CuK_α radiation was generated at 40 kV and 30 mA. Samples were scanned from 15–75(2θ) at a rate of 5 s per step for all porous manganese oxide-doped titania samples. Brunauer-Emmett-Teller (BET) surface area of all samples was obtained at 77 K using the Quantachrome (Model 1987) instrument. All the samples were degassed at 573 K for 12 h. The instrument used for nitrogen adsorption analysis is NOVA 2000 from Quantachrome Corporation. The morphology and elemental analysis of the catalyst (average of five data points at different locations of the solid) were measured by energy dispersive X-ray spectroscopy (EDX) and standard deviation of the corresponding element is measured. Scanning electron microscopy (SEM) images were captured using JEOL-JSM 5310 model instrument connected to EDX. Transmission electron microscopy (TEM) was examined using Philips CM12/STEM, Scientific and Analytical Equipment. The particle size distributions were determined by a Coulter LS230 laser granulometer with a particle measurement range of 0.4–2000 μm. All samples were prepared in suspension form and thoroughly mixed suspension was poured into the pouring chamber of the laser granulometer.

Catalysts Preparation

Potassium birnessite (K-OL-1) was synthesized via $Mn(OH)_2$ suspension formation and oxidized by potassium permanganate, the detailed procedure has been reported elsewhere [16]. K-OMS-2 type porous manganese oxide was synthesized by redox reaction between manganese(II) sulfate and potassium permanganate. The MnO_4^-/Mn^{2+} ratio was fixed at 0.76 for preparing cryptomelane type K-OMS-2 material in acidic medium and the detailed procedure has been reported elsewhere [17, 22]. The synthesized K-OMS-2 was calcined in air at 723 K for 4 h to test the catalyst activity. The 5 wt % K-OL-1/TiO_2 and 5 wt % K-OMS-2/TiO_2 catalysts were prepared by doping of 2.0 g of titanium dioxide with o.1 g of bulk K-OL-1 and K-OMS-2 by wet impregnation method. After stirring, the porous manganese oxide (K-OL-1 and K-OMS-2) doped TiO2 was then calcined at 723 K for 4 h. The synthesized porous manganese oxide-doped TiO_2 and calcined commercial TiO_2 catalysts are uti-

lized to test the catalytic activity for dye degradation and phenol decomposition.

Catalytic Activity Test and Analysis

Methylene blue dye degradation (50 ml of 50 mg/l) was added to a 100-ml plastic beaker with 0.1 g of catalyst and ultrasonicated directly at 600 W ultrasonicator. In case of phenol decomposition reaction test, 50 ml of aqueous phenol solution (50 mg/l) were added to a 100-ml plastic beaker with 0.1 g of catalyst and the solution pH was adjusted to 3.5 using 0.1 M NaOH or 0.1 M HCl, followed by direct ultrasonication (Sonicator 3000, Misonix, USA, output power of 600 W) in the presence of catalysts for 30 min. For the mixed ultrasonication experiment, the reactant solution was first ultrasonicated by an ultrasonic cleaner (BRANSON 3210, output power of 120 W) for 100 min, followed by direct ultrasonication for 30 minutes. The pH value for all phenol removal experiments were adjusted to 3.5 and monitored by a pH-stat (TIM865 titration manager).

After 30 min of direct ultrasonic irradiation, suitable amount of reacted solution was removed by filtration using a 0.45-μm MILLEX HA millipore membrane filter for analysis. Dye degradation rate of the reactant solution was scanned by UV-Vis spectrometer (GBC Cintra 6) in the wavelength range between 700–200 nm after the catalytic ultrasonic irradiation. After the catalytic ultrosonication process, phenol concentration in the reactant solution was determined by an UV-Vis spectrometer at fixed wavelength of 272 nm in 0.005 M sodium nitrate solution by standard calibration method.

RESULTS AND DISCUSSION

X-Ray Diffraction Study

X-ray diffraction patterns of K-OL-1- and K-OMS-2-doped TiO_2 materials are shown in Fig. 1. Porous manganese oxide-doped TiO_2 samples showed the major phase of anatase with trace amount of the rutile phase. The major peak at 25.3° 2θ and *d*-spacing of 3.52 Å (100) of anatase (intense peak) are observed for all samples. According to our previous reports, porous manganese oxide is found to be well dispersed on the support surface like Mn^{2+} species, while some of the manganese with higher valence was stabilized with the TiO_2 lattice like Mn^{4+} species [23]. Specific *d*-space value for K-OL-1 or K-OMS-2 phase was not observed in the XRD patterns, due to lower loading or dispersion of manganese in bulk support of TiO_2. XRD patterns of bulk K-OL-1 and K-OMS-2 have been reported elsewhere [16, 22].

Particle Size Measurements of As-Synthesized Catalysts

The particle size measurement of porous manganese oxide-doped TiO_2, bulk K-OMS-2 and TiO_2 samples are shown in Table 1. As can be seen, compared with that of bulk TiO_2, the particle size increased after doping the porous manganese oxide into TiO_2 lattice. Table 1 also shows the surface area of the corresponding samples and the details are given below.

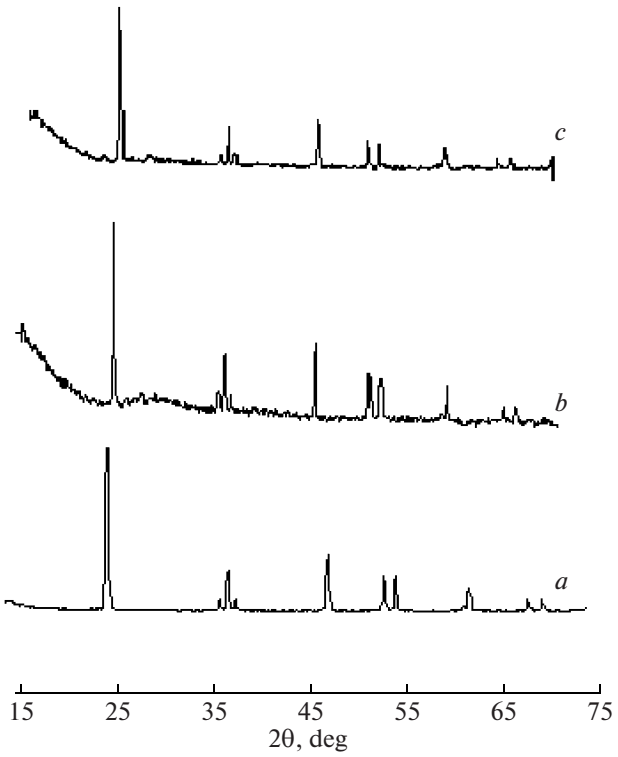

Fig. 1. X-ray diffraction patterns of (*a*) TiO_2, and manganese oxide-doped titania (*b*) 5 wt % K-OL-1/TiO_2 and (*c*) 5 wt % K-OMS-2 /TiO_2.

Textural Characterization of As-Synthesized Catalysts

Transmission electron micrographs of 5 wt % K-OMS-2/TiO_2 are shown in Figs. 2a, 2b and K-OMS-2 type porous manganese oxide forms the disordered aggregated particle formation with TiO_2. Titania particles of spherical and thin platy morphology can be

Table 1. Particle size measurements and BET surface area of synthesized catalysts

Catalyst	Particle size, μm	BET surface area, m^2/g
K-OL-1	0.51	31
K-OMS-2	0.52	48
TiO_2	0.46	36
5 wt % K-OL-1/TiO_2	0.47	37
5 wt % K-OMS-2/TiO_2	0.46	41

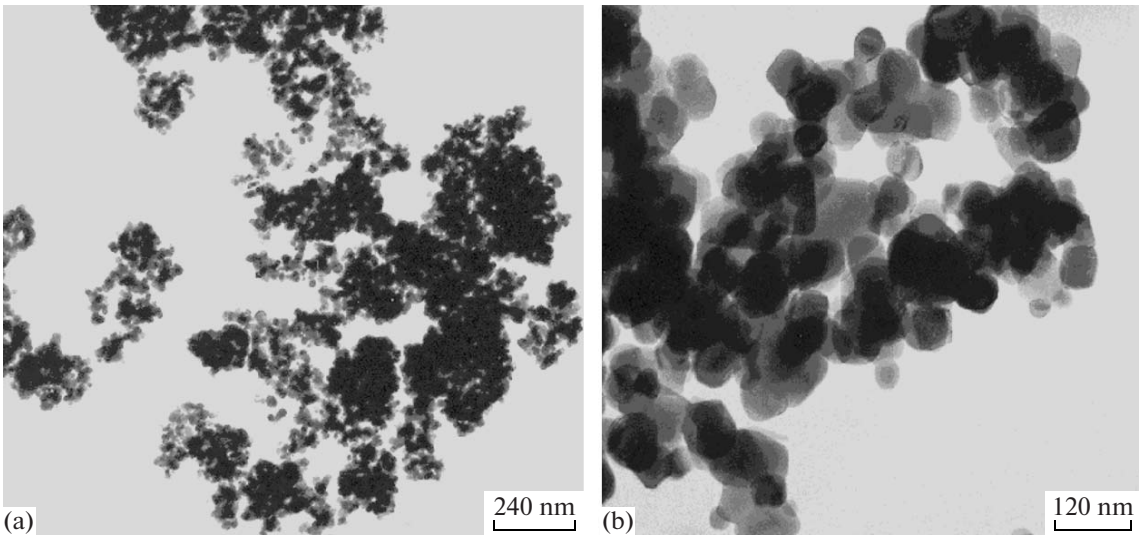

Fig. 2. Transmission electron micrographs of 5 wt % K-OMS-2/TiO_2. (a) ×16000 magnification and (b) ×24000 magnification.

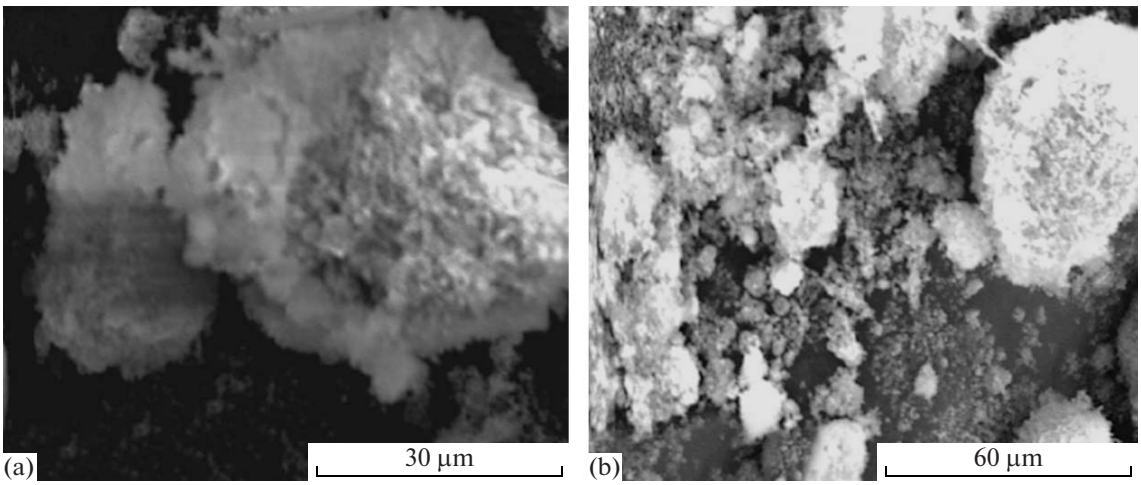

Fig. 3. Scanning electron micrographs of 5 wt % K-OMS-2/TiO_2. (a) ×16000 magnification and (b) ×24000 magnification.

clearly observed at high resolution (Fig. 2b). The picture of porous manganese oxide-doped TiO_2 of lower magnification clearly indicates the aggregated particle morphology of K-OMS-2-doped TiO_2 (Fig. 2a). The corresponding elemental composition for 5 wt % K-OMS-2-doped TiO_2 is 0.4 at % for Mn and 81 at % for Ti. The SEM micrographs of 5 wt % K-OMS-2 doped TiO_2 (Fig. 3) indicates the formation of aggregated particle morphology with spherical shape particle morphology. BET surface area of as synthesized catalysts are shown in Table 1. The surface areas of 5 wt % K-OL-1-doped TiO_2, 5 wt % K-OMS-2 doped TiO_2, and K-OMS-2 are 37, 41, and 48 m^2/g, respectively. The BET surface area of porous manganese oxide-doped titania is greater than that of pure TiO_2 due to dispersion of porous manganese oxide on TiO_2. Porosity of the dispersed species on the external surface of fine TiO_2 causes increase in surface area. Our previous report suggested that difference in preparation method has accounted for the greater surface area of porous manganese oxide-doped titania in aqueous medium, compared with that doped in alcohol medium [19].

Ultrasonication-Assisted Catalytic Activity Test

Figures 4 and 5 show the methylene blue dye degradation efficiency of as synthesized titanium dioxide and porous manganese oxide-doped TiO_2 composite catalyst in the presence of ultrasonic irradiation. Figure 4 shows the efficiency of methylene blue dye degradation on TiO_2 catalyst of different weights in the presence of high-power-assisted ultrasonication. Three absorbance peaks with a small shoulder peak was observed for methylene blue dye degradation. In

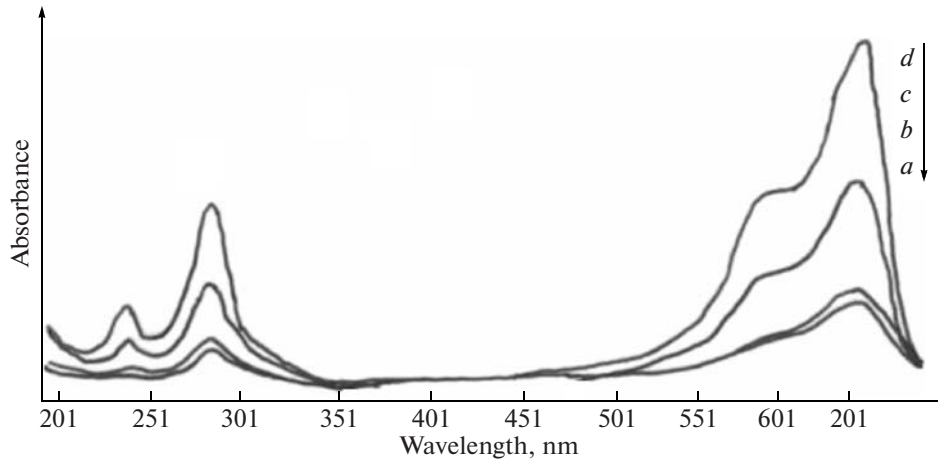

Fig. 4. Dye degradation efficiency of TiO_2: *a*—0.2 g of TiO_2 at power level of 8, *b*—0.1 g of TiO_2 at power level of 8, *c*—0.1 g of TiO_2 at power level of 4, and *d*—50 mg/L of methylene blue ultrasonicated without catalysts at power level of 8.

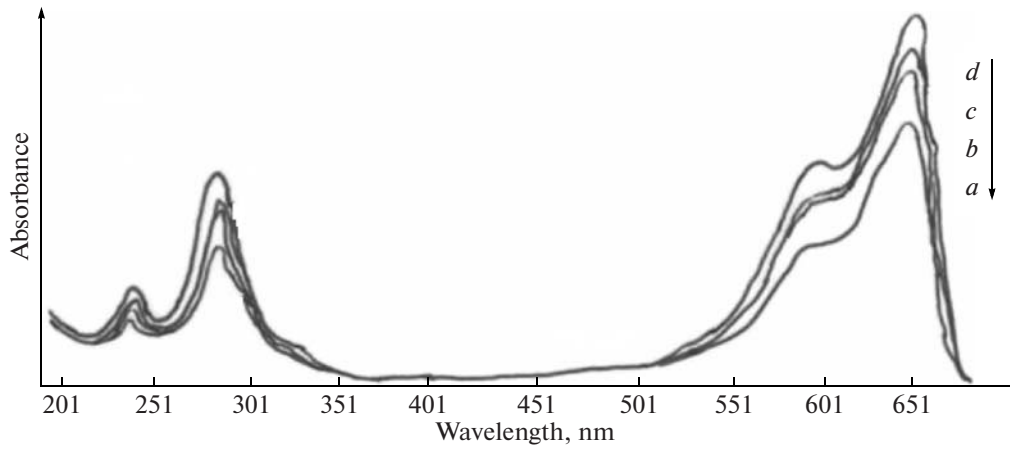

Fig. 5. Dye degradation efficiency of TiO_2 and porous manganese oxide-doped TiO_2 catalysts: *a*—0.1 g of TiO_2, *b*—5 wt % K-OMS-2/TiO_2, *c*—5 wt % K-OL-1/TiO_2, and *d*—50 mg/L of methylene blue ultrasonicated without catalyst at power level of 8.

general, methylene blue in aqueous solution show three major absorbance peaks at 246, 295, and 665 nm. Both 0.2 and 0.1 g of TiO_2 (Fig. 4, curves *a*, *b*) show higher degradation efficiency at power level of 8 (power level 8 produces 66 W at a fixed 10 s pulse-on time). Figure 4, curve *c* shows the methylene blue dye degradation at power level of 4 (power level 4 corresponds to 36 W at pulse-on time of 10 s and pulse-off time of 15 s). Figure 4, curve *d* shows the original dye degradation rate of ultrasound irradiation without catalyst. The effects of amount of catalysts used and ultrasonic power level or intensity for methylene blue dye degradation have been studied in the presence of ultrasonication. Wang et al. [24] have recently studied the sonocatalytic activity of synthesized nanocrystals of TiO_2 powders for methylene blue dye degradation using a lower output power ultrasonic cleaner sonicator for 1 to 3 h. They found that longer reaction time of ultrasonic irradiation (3 h) results in more efficient dye degradation.

In the present experiment, high-power-assisted direct ultrasonication is applied for methylene blue degradation. Results obtained show higher, cheaper and more efficient dye degradation achieved under short reaction duration of 30 min in the presence of calcined TiO_2 at power level of 8. Figure 5 shows the dye degradation efficiency for K-OL-1 and K-OMS-2-doped TiO_2 as well as TiO_2 alone. The dye degradation efficiency follows the order: TiO_2 > 5 wt % K-OMS-2/TiO_2 > 5 wt % K-OL-1/TiO_2 (Fig. 5, curves *a*–*c*). Figure 5, curve *d* shows the original dye degradation rate under ultrasound irradiation without catalyst. TiO_2 alone performed better compared with porous manganese oxide-doped titania catalysts in ultrasonic-assisted dye degradation at power level of 8 and 30 min reaction time due to the fine particle size and ordered surface morphology of TiO_2. Doping of

Table 2. Phenol removal efficiency in the presence of catalysts at direct high-power-assisted ultrasonication and mixed ultrasonication processes

Catalyst	Direct ultrosonication (30 min at 600 W power). Phenol removal, %	Mixed ultrosonication (100 min at 120 W + 30 min at 600 W). Phenol removal, %
K-OL-1	2.00	3.20
K-OMS-2	31.77	58.40
TiO_2	22.00	9.80
5 wt % K-OL-1/TiO_2	3.00	4.50
5 wt % K-OMS-2/TiO_2	14.00	45.00

porous manganese oxide increases the particle size, and increase in particle size of K-OL-1/TiO_2 and K-OMS-2/TiO_2 catalyst hinders the formation of radicals in intermediate catalytic dye degradation during ultrasonication, which results in a lower dye degradation rate, compared with that of bulk TiO_2.

Lachheb et al. [25] reported the details of reaction products of different dyes degradation reactions. SO_4^{2-} is the initial product of methylene blue due to OH radical attack at sulfonyl group. Ammonium and nitrate nitrogen other degradation products. Lachheb et al. tested the different dye degradation on commercial P25 TiO_2. The concentration of above mentioned products are observed below the expected values even at longer time duration (1400 min). Sulphate concentration observed below 85 μmol/l and total Nitrogen ($NO_3^- + NH_4^+$) concentration below 390 μmol/l until 1400 min. The concentration of degradation product is below the expected hazardous level and hazardous degradation product follow the order $NH_4^+ < NO_3^- < SO_4^{2-}$ [25].

Table 2 shows the phenol removal efficiency achieved by direct ultrasonication and mixed ultrasonication in the presence of catalysts. Phenol removal efficiency of direct ultrasonication in the presence of catalyst follows the order: K-OMS-2 > TiO_2 > K-OMS-2/TiO_2 > K-OL-1/TiO_2 (Table 2). Bulk K-OMS-2 is a more suitable catalyst for phenol sorption and removal experiment compared with bulk K-OL-1 due to its surface acid-base property. Bulk K-OL-1 shows negligible activity of phenol removal by ultrasonication. K-OMS-2 and titania catalysts show more efficient phenol removal efficiency achieved by direct ultrasonication process compared with porous manganese oxide-doped titania catalyst because fewer radicals were formed within the short reaction duration. As for the mixed ultrasonication process, both K-OMS-1- and K-OMS-2-doped titania show better and more promising phenol removal efficiency with good reproducibility compared with TiO_2 and K-OL-1/TiO_2. Reproducibility of phenol removal efficiency for TiO_2 and K-OL-1/TiO_2 catalyst are not promising in the ultrasonication process due to the surface acid-base property of bulk TiO_2 and the nature of the catalyst surface. Hence, K-OL-1/TiO_2 and TiO_2 alone show reduced activity due to poor activation of catalyst surface within the short reaction duration and low ultrasonic power level. K-OMS-2 and K-OMS-2/TiO_2 catalyst are effective in activating the formation of surface species because the presence of active oxygen species in manganese oxide lattice and perfect phenol sorption facilitate the formation of radicals for the phenol decomposition process. The presence of K-OMS-2 and K-OMS-2/TiO_2 catalyst, optimal ultrasonic power level of 8 and pH of 3.5 are perfect reaction conditions for removal of phenol compounds by ultrasonication.

CONCLUSIONS

The promising K-OMS-2 and K-OMS-2-doped TiO_2 sonocatalysts are prepared by aqueous impregnation method. The aggregated particle morphology was observed for 5 wt % K-OMS-2-doped TiO_2 and the particle formed had spherical and platy morphology. The 5 wt % K-OMS-2-doped titania shows greater surface area than bulk TiO_2. Methylene blue dye degradation rate improved by optimal amount of pure TiO_2 catalyst compared to manganese oxide doped TiO_2 composite powder at ultrasonication process. K-OMS-2 and K-OMS-2/TiO_2 are showing good and promising results for efficient phenol decomposition under optimized ultrasonic reaction conditions (power level 8 and pH 3.5 of the reactant solution). Experimental results of the present study predict that the photo-ultrasonication process in the presence of K-OMS-2/TiO_2 catalyst offer an economic and efficient approach to phenol decomposition or removal process in industrial waste water treatment.

ACKNOWLEDGMENTS

We express the sincere thanks to the National Science Council of Taiwan (NSC-95-2811-Z-002-005) for financial support.

REFERENCES

1. Destaillats, H., Hung, H.M., and Hoffmann, M.R., *Environ. Sci. Technol.*, 2000, vol. 34, p. 311.
2. Nagata, Y., Nakagawa, M., Okuno, H., Mizukoshi, Y., Yim, B., and Maeda, Y., *Ultrason. Sonochem.*, 2000, vol. 7, p. 115.
3. Stavarache, C., Yim, B., Vinatoru, M., and Maeda, Y., *Ultrason. Sonochem.*, 2002, vol. 9, p. 291.

4. Suslick, K.S., in *Ultrasound: Its Chemical, Physical and Biological Effects*, Suslick, K.S., Ed., New York: VCH, 1988.
5. Suslick, K.S., *Science*, 1990, vol. 247, p. 1439.
6. Suslick, K.S., Hammerton, D.A., and Cline, R.E., *J. Am. Chem. Soc.*, 1986, vol. 108, p. 5641.
7. Shutilov, V.A., *Fundamental Physics of Ultrasound*, New York: Gordon & Breach, 1988.
8. Li, M., L J.T.I, Sun H.W, *Ultroson. Sonochem.*, 2008, vol. 15, p. 37.
9. Suslick, K.S. and Price, G.J., *Annu. Rev. Mater. Sci.*, 1999, vol. 29, p. 295.
10. Dvoranová, D., Brezová, V., Mazúra, M., and Malati, M.A., *Appl. Catal., B*, 2002, vol. 37, p. 91.
11. Arroyo, R., Cordoba, G., Padilla, J., and Lara, V.H., *Mater. Lett.*, 2002, vol. 54, p. 397.
12. Boreskov, G.K., in *Catalysis Science and Technology*, Anderson, J.R. and Boudart, M., Eds., Berlin: Springer, 1982, vol. 3.
13. Luo, J., Zhang, Q., Huang, A., and Suib, S.L., *Microporous Mesoporous Mater.*, 2000, vols. 35–36, p. 209.
14. Ramesh, K., Chen, L., Chen, F., Liu, Y., Wang, Z., and Han, Y.F., *Catal. Today*, 2008, vol. 131, p. 477.
15. Kapteijn, F., Singoredjo, L., van Driel, M., Andreini, A., Moulijn, J.A., Ramis, G., and Busca, G., *J. Catal.*, 1994, vol. 150, p. 105.
16. Jothiramalingam, R., Viswanathan, B., and Varadarajan, T.K., *Mater. Chem. Phys.,* 2006, vol. 100, p. 257.
17. Yin, Y.G., Xu, W.Q., DeGuzman, R., Suib, S.L., and O'Young, C.L., *Inorg. Chem.*, 1994, vol. 33, p. 4384.
18. Post, J.E. and Veblen, D.R., *Am. Mineral.*, 1990, vol. 75, p. 477.
19. Jothiramalingam, R. and Wang, M.K., *J. Hazard. Mater.*, 2007, vol. 147, p. 562.
20. Carvalho, C., Fernandes, A., Lopes, A., Pinheiro, H., and Goncalves, I., *Chemosphere*, 2007, vol. 67, p. 1316.
21. Dincer, A.R., Gunes, Y., and Karakaya, N., *J. Hazard. Mater.*, 2007, vol. 141, p. 529.
22. Jothiramalingam, R., Viswanathan, B., and Varadarajan, T.K., *Catal. Commun.*, 2005, vol. 6, p. 41.
23. Gallardo-Amores, J.M., Armaroli, T., Ramis, G., Finocchio, E., and Busca, G., *Appl. Catal., B*, 1999, vol. 22, p. 249.
24. Wang, J., Sun, W., Zhang, Z., Xing, Z., Xu, R., Li, R., Li, Y., and Zhang, X., *Ultroson. Sonochem.*, 2008, vol. 15, p. 301.
25. Lachheb, H., Puzenat, E., Houas, A., Ksibi, M., Elaloui, E., Guillard, C., and Herrmann, J.M., *Appl. Catal., B*, 2002, vol. 39, p. 75.